Ethylene Polymerization Behavior of Tris(pyrazolyl)borate Titanium(IV) Complexes

Shahid Murtuza,[†] Osvaldo L. Casagrande, Jr.,[‡] and Richard F. Jordan*,[†]

Department of Chemistry, The University of Chicago, 5735 South Ellis Avenue, Chicago, Illinois 60637, and Laboratório de Catálise Molecular, Instituto de Quimica-Universidade Federal do Rio Grande do Sul, Avenida Bento Goncalves, 9500, Porto Alegre, RS, 90501-970, Brazil

Received June 18, 2001

A set of Tp′$TiCl_3$ and Tp′$TiCl_2$(OR) complexes containing tris(pyrazolyl)borate ligands with diverse steric properties has been evaluated for ethylene polymerization under MAO activation conditions (Tp′ = HB(3-mesitylpyrazolyl)$_2$(5-mesitylpyrazolyl)$^-$ (Tp^{Ms*}), HB(3-mesitylpyrazolyl)$_3^-$ (Tp^{Ms}), HB(3,5-Me_2-pyrazolyl)$_3^-$ (Tp^*), HB(pyrazolyl)$_3^-$ (Tp), BuB(pyrazolyl)$_3^-$ (^{Bu}Tp)). The activity of Tp′TiX_3/MAO varies in the order $Tp^{Ms*}TiCl_3$ (**10c**) > $Tp^{Ms}TiCl_3$ ≫ Tp^*TiCl_3, $TpTiCl_3$, $^{Bu}TpTiCl_3$, Tp*$TiCl_2$(O^{t}Bu), Tp*$TiCl_2$(O-2-^{t}Bu-C_6H_4). The activity of **10c**/MAO is similar to that of Cp_2ZrCl_2/MAO. High MAO levels or addition of $AlMe_3$ decrease the activity of **10c**/MAO, probably due to coordination of $AlMe_3$ to the active Ti species. The predominant chain transfer mechanism for **10c**/MAO is chain transfer to $AlMe_3$, which results in broad molecular weight distributions at low Al/Ti ratios (Al/Ti = 200−1000). At *very* high Al levels (**10c**/5000 MAO or **10c**/1000 MAO/4000 $AlMe_3$) bimodal molecular weight distributions comprising a major low molecular weight fraction (M_w/M_n ca. 3) and a minor high molecular weight fraction are observed, which suggests that several active species are present, only one of which undergoes efficient chain transfer to Al.

Introduction

Several important classes of olefin polymerization catalysts based on discrete titanium complexes activated by methylalumoxane (MAO) or boron-based cocatalysts have been developed that exhibit unique properties. Among the most notable of these single-site titanium catalysts are ($C_5R_4SiMe_2NR$)TiX_2/activator catalysts (**1**, Chart 1), which exhibit unprecedented scope for the copolymerization of α-olefins, styrenes, and even isobutylene with ethylene,[1] (Ar$NCH_2CH_2CH_2NAr$)TiX_2/activator catalysts (**2**), which polymerize 1-hexene in a "living" fashion,[2] (C_5R_5)TiX_3/activator catalysts (**3**), which polymerize styrene to syndiotactic polymer with high activity and stereoselectivity,[3] and ($R_3P{=}N)_2TiX_2$/activator catalysts (**4**), which polymerize ethylene with extraordinarily high activity at high temperatures.[4] These advances have prompted studies of titanium catalysts containing a wide variety of ancillary ligands,

Chart 1

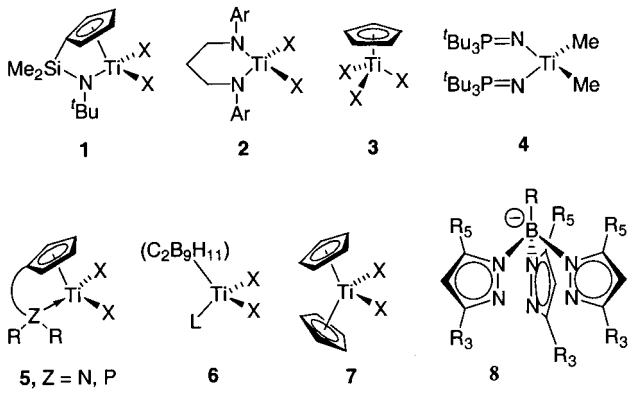

including, for example, cyclopentadienyl ligands with pendant neutral donor groups (**5**),[5] carboranyl ligands (**6**),[6] amidopyridinates,[7] and mixed cyclopentadienyl-

[†] The University of Chicago.
[‡] Universidade Federal do Rio Grande do Sul.

(1) (a) Canich, J. A. M.; Turner, H. W. PCT Appl. WO 92 12162, 1992 (*Chem. Abstr.* **1993**, *118*, 81615j). (b) Stevens, J. C.; Timmers, F. J.; Wilson, D. R.; Schmidt, G. F.; Nickias, P. N.; Rosen, R. K.; Knight, G. W.; Lai, S.-Y. Eur. Pat. Appl. 0 416 815, 1990 (*Chem. Abstr.* **1991**, *115*, 93163m). (c) Chen, Y.-X.; Marks, T. J. *Organometallics* **1997**, *16*, 3649. (d) McKnight, A. C.; Waymouth, R. M. *Chem. Rev.* **1998**, *98*, 2578. (e) Shaffer, T. D.; Cannich, J. A. M.; Squire, K. R. *Macromolecules* **1998**, *31*, 5145.

(2) (a) Scollard, J. D.; McConville, D. H.; Payne, N. C.; Vittal, J. J. *Macromolecules* **1996**, *29*, 5241. (b) Scollard, J. D.; McConville, D. H.; Vittal, J. J.; Payne, N. C. *J. Mol. Catal. A* **1998**, *128*, 201.

(3) (a) Tomotsu, N.; Ishihara, N.; Newman, T. H.; Malanga, M. T. *J. Mol. Catal. A* **1998**, *128*, 167. (b) Pellecchia, C.; Grassi, A. *Top. Catal.* **1999**, *7*, 125. (c) Tomotsu, N.; Ishihara, N. *Stud. Surf. Sci. Catal.* **1999**, *121*, 269. (d) Ishihara, N.; Kuramoto, M.; Uoi, M. *Macromolecules* **1988**, *21*, 3356.

(4) (a) Stephan, J. D.; Guérin, F.; Spence, R. E. v. H.; Koch, L.; Gao, X.; Brown, S. J.; Swabey, J. W.; Wang, Q.; Xu, W.; Zoricak, P.; Harrison, D. G. *Organometallics* **1999**, *18*, 2046. (b) Brown, S. J.; Gao, X.; Harrison, D. G.; McKay, I.; Koch, L.; Wang, Q.; Xu, W.; Von Hakken Spence, E. R.; Stephan, D. W. PCT Appl. WO 000 5238, 2000.

(5) (a) van Beek, J. A. M.; van Doremaele, G. H. J.; Gruter, G. J. M.; Arts, H. J.; Eggels, G. H. M. R. PCT Appl. WO 96 13529, 1996. (b) van Beek, J. A. M.; van Doremaele, G. H. J.; Gruter, G. J. M.; Arts, H. J.; Eggels, G. H. M. R. Eur. Pat. Appl. EP 0 789 718, 1997. (c) van Beek, J. A. M.; van Doremaele, G. H. J.; Gruter, G. J. M.; Arts, H. J.; Eggels, G. H. M. R. U.S. Patent 5 986 029, 1999. (d) Gruter, G. J. M.; Kranenburg, M.; Herklots, M. Eur. Pat. App. EP 0 919 571, 1999.

(6) (a) Saccheo, S.; Gioia, G.; Grassi, A.; Bowen, D. E.; Jordan, R. F. *J. Mol. Catal. A* **1998**, *128*, 111. (b) Kim, I.; Nishihara, Y.; Jordan, R. F.; Rogers, R. D.; Rheingold, A. L.; Yap, G. P. A. *Organometallics* **1997**, *16*, 3314.

(7) Fuhrmann, H.; Brenner, S.; Arndt, P.; Kempe, R. *Inorg. Chem.* **1996**, *35*, 6742.

10.1021/om010530j CCC: $22.00
Publication on Web 03/28/2002

alkoxide ligands.[8] In contrast, Cp_2TiX_2/activator catalysts (**7**) generally exhibit poor performance due to rapid deactivation via reduction to Ti^{III} species.[9]

Tris(pyrazolyl)borates (Tp′, **8**, Chart 1) are attractive candidates for ancillary ligands in discrete titanium catalysts because they coordinate strongly to early transition metals in a tridentate fashion, the hard N-donor groups may stabilize Ti^{IV} species against reduction, and the steric and electronic properties of the pyrazolyl donors can be modified by variation of the 3 and 5 substituents.[10] Several studies have demonstrated that Tp′$TiCl_3$/MAO catalysts containing the simple Tp′ ligands HB(pyrazolyl)$_3^-$ (Tp) or HB(3,5-dimethylpyrazolyl)$_3^-$ (Tp*) polymerize ethylene, ethylene/α-olefins, and styrene.[11,12] However, these catalysts exhibit poor activity and produce polymers with broad molecular weight distributions, and few data are available concerning the nature of the active species. Mixed Cp Tp′ catalysts (C_5R_5)(Tp′)$TiCl_2$/MAO (Tp′ = Tp or Tp*) are more active than Tp′$TiCl_3$/MAO for ethylene polymerization.[11g]

To date, studies in this area have been limited to Tp and Tp* ligands, and little is known about how the Tp′ structure may influence catalyst performance. It may be anticipated that use of other Tp′ ligands, particularly sterically bulky examples, may lead to more active catalysts and interesting polymerization behavior. With this possibility in mind, we have initiated studies of Tp′TiX_3/MAO catalysts which incorporate a range of sterically diverse Tp′ ligands. Here, we describe the syntheses of Tp′TiX_3 complexes which incorporate bulky substituents in the pyrazolyl 3 or 5 positions, the identification of specific Tp′ ligands that result in high ethylene polymerization activity for this catalyst class, and studies of the chain transfer processes in ethylene polymerization by these catalysts.

Results and Discussion

Synthesis and Characterization of Tp′$TiCl_3$ Complexes. Alkali metal or Tl^I salts of the Tp′ ligands used in this work (**9a**−**e**, eq 1) were prepared by literature procedures.[13] These ligands were chosen for their diverse steric properties, which range from relative steric compactness (Tp, ^{Bu}Tp) to a high degree of crowding (Tp^{Ms}). In addition, the ^{Bu}Tp ligand, which features a B−Bu group in place of the standard B−H unit, was utilized to probe possible involvement of the B−H group in catalysis.

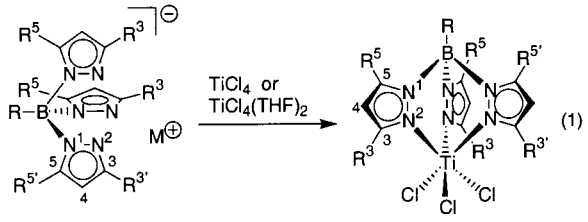

(1)

9a-e **10a-e**

	ligand	M	R	R^3	$R^{3'}$	R^5	$R^{5'}$
a	Tp*	K	H	CH_3	CH_3	CH_3	CH_3
b	Tp^{Ms}	Tl	H	Ms[a]	Ms	H	H
c	Tp^{Ms*}	Tl	H	Ms	H	H	Ms
d	^{Bu}Tp	Na	Bu	H	H	H	H
e	Tp	K	H	H	H	H	H

[a] Ms = 2,4,6-trimethylphenyl.

Tp*$TiCl_3$ (**10a**) and Tp$TiCl_3$ (**10e**) were prepared by the reaction of KTp* or KTp with $TiCl_4$ using modified literature procedures.[14] The B−Bu derivative ^{Bu}Tp$TiCl_3$ (**10d**) was prepared in 70% yield by the reaction of Na[^{Bu}Tp] (**9d**) with 1 equiv of $TiCl_4$ in CH_2Cl_2.

The reaction of **9b** with 1 equiv of $TiCl_4$ in CH_2Cl_2 at room temperature affords Tp$^{Ms}TiCl_3$ (**10b**), which is isolated as an orange solid (67%, Scheme 1). In contrast, the reaction of **9b** with $TiCl_4$ or $TiCl_4(THF)_2$ in THF yields the isomer Tp$^{Ms*}TiCl_3$ (**10c**), which is isolated as a yellow solid (65%). Interestingly, the reaction of **9b** with $TiCl_4(THF)_2$ in CH_2Cl_2 yields a 96/4 mixture of **10c**/**10b**, from which **10c** is easily separated due to its higher solubility in polar solvents. Thus the presence of even a small amount of THF results in formation of the isomerized product. Compound **10c** can also be prepared in 70% yield by the reaction of **9c** with 1 equiv of $TiCl_4$ in CH_2Cl_2.

Scheme 1

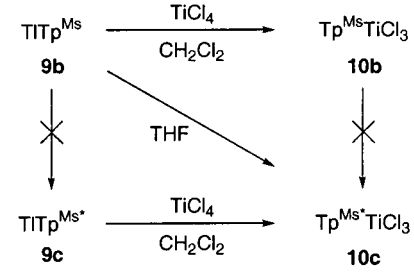

Isomers **10b** and **10c** are related by a net 1,2-borotropic shift which exchanges the 3- and 5-positions of one pyrazolyl ring. Isomerizations of this type are well-documented and can occur when bulky substituents are present at the pyrazolyl 3-positions.[15] In principle, the starting Tl complex **9b**, the product **10b**, or an

(8) Chen, Y.-X.; Fu, P.-F.; Marks, T. J. *Organometallics* **1997**, *16*, 5958.

(9) (a) Breslow, D. S.; Newburg, N. R. *J. Am. Chem. Soc.* **1959**, *81*, 81. (b) Chien, J. C. W. *J. Am. Chem. Soc.* **1959**, *81*, 86. However, see: (c) Ewen, J. A.; Zambelli, A.; Longo, P.; Sullivan, J. M. *Macromol. Rapid Commun.* **1998**, *19*, 71.

(10) (a) Trofimenko, S. *Scorpionates: The Coordination Chemistry of Polypyrazolylborate Ligands*; Imperial College Press: London, 1999. (b) Parkin, G. *Adv. Organomet. Chem.* **1995**, *42*, 291. (c) Kitajima, N.; Tolman, W. B. *Prog. Inorg. Chem.* **1995**, *43*, 419. (d) Trofimenko, S. *Chem. Rev.* **1993**, *93*, 943.

(11) (a) Nakazawa, H.; Ikai, S.; Imaoka, K.; Kai, Y.; Yano, T. *J. Mol. Catal. A* **1998**, *132*, 33. (b) Obara, T.; Ueki, S. Jpn. Kokai Tokkyo Koho 01 095 110, 1989. (c) Jens, K. J.; Tilset, M.; Heuman, A. PCT Int. Appl. WO 97 17379, 1997. (d) Matsunaga, P. T.; Rinaldo, S. PCT Int. Appl. WO 99 29739, 1999. (e) Ikai, S.; Kai, Y.; Murakami, M.; Nakazawa, H. Jpn. Kokai Tokkyo Koho 11 228 614, 1999. (f) Newman, T. H. Eur. Pat. Appl. 0 482 934, 1992. (g) Aoki, T.; Kaneshima, T. Eur. Pat. Appl. 0 617 052, 1994.

(12) For olefin polymerization with Cp′Tp′ZrX_2 catalysts (Cp′ = C_5H_5 or C_5Me_5; Tp′ = Tp, Tp*, ^{Bu}Tp (^{Bu}Tp = Bu−B(pyrazolyl)$_3$)), see: (a) Wang, S.-J.; Chen, Y.-C.; Chain, S.-H.; Tsai, J.-C.; Sheu, Y.-H. E. U.S. Patent 5 519 099, 1999. (b) Yorisue, T.; Kanejima, S. Jpn. Kokai Tokkyo Koho 08 027 210, 1996. (c) Matsushita, F.; Yamaguchi, F.; Izuhara, T. Jpn. Kokai Tokkyo Koho 08 059 746, 1996.

(13) (a) Reger, D. L.; Tarquini, M. E. *Inorg. Chem.* **1982**, *21*, *840*. (b) Trofimenko, S. *J. Am. Chem. Soc.* **1967**, *89*, 6288. (c) Rheingold, A. L.; White, C. B.; Trofimenko, S. *Inorg. Chem.* **1993**, *32*, 3471.

(14) Kouba, J. K.; Wreford, S. S. *Inorg. Chem.* **1976**, *15*, 2313.

(15) (a) Reinaud, O. M.; Rheingold, A. L.; Theopold, K. H. *Inorg. Chem.* **1994**, *33*, 2306. (b) Calabrese, J. C.; Trofimenko, S. *Inorg. Chem.* **1992**, *31*, 4810. (c) Looney, A.; Parkin, G. *Polyhedron* **1990**, *9*, 265. (d) Trofimenko, S.; Calabrese, J. C.; Domaille, P. J.; Thompson, J. S. *Inorg. Chem.* **1989**, *28*, 1091.

Scheme 2

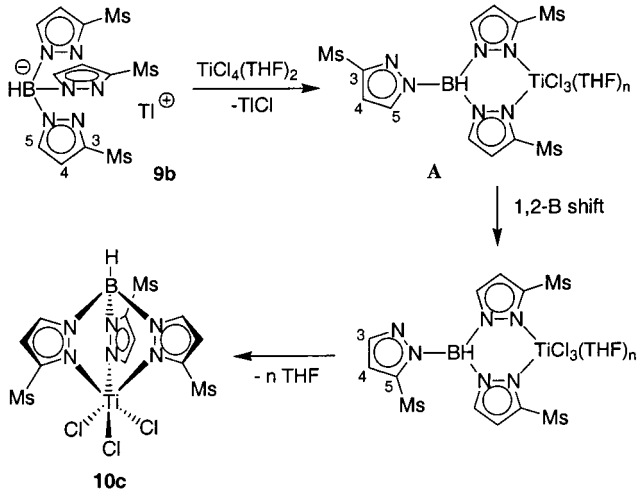

intermediate could undergo isomerization.[16] However, neither **9b** nor **10b** isomerizes in THF-d_8 solution at 23 °C or after 2 days at 50 °C (Scheme 1), which suggests that an intermediate undergoes the isomerization. A plausible mechanism is shown in Scheme 2. In this process, coordination of the pendant 3-mesitylpyrazolyl group of intermediate **A** is inhibited by steric crowding and does not occur until the 1,2-borotropic shift converts this ring to the more nucleophilic 5-mesitylpyrazolyl group. In the absence of THF, the intermediates may be less highly solvated and thus more electrophilic at Ti, and coordination of all three pyrazolyl rings may occur without isomerization. Similar solvent effects were observed in studies of the reaction of $TiCl_4$ with the bulky reagent $TlTp^{Menth}$.[17]

The ^{1}H NMR spectrum of **10c** (see Figure 1 for labeling scheme) is consistent with the proposed C_s-symmetric structure. This spectrum contains two sets of pyrazolyl resonances (two doublets for each set) in a 1:2 intensity ratio for the unique 5-mesitylpyrazolyl group ($H^{a'}$, $H^{b'}$) and the two equivalent 3-mesitylpyrazolyl groups (H^a, H^b). Due to restricted rotation around the pyrazolyl−mesityl bonds, the mesityl *ortho* methyl groups of the 3-mesitylpyrazolyl groups are separated into "outer" (Me^c) and "inner" (Me^d) sets with respect to the symmetry plane that runs through the 5-mesitylpyrazolyl group. Thus, the spectrum contains five mesityl methyl resonances in a 6:6:6:6:3 (Me^c:Me^d:Me^e:Me^f:Me^g) intensity ratio. The ^{1}H NMR spectrum of **10b** is consistent with the proposed C_{3v}-symmetric structure in which the three 3-mesitylpyrazolyl groups are equivalent. This spectrum contains one set of pyrazolyl resonances (two doublets in a 3:3 intensity ratio) and two singlets for the mesityl methyl groups (18:9 intensity ratio). Rotation around the mesityl−pyrazolyl bonds of **10b** is undoubtedly restricted as in **10c**, but this feature cannot be detected by NMR due to the symmetry of the complex.

The alkoxide derivative Tp*Ti(O^{t}Bu)Cl_2 (**11a**) was previously prepared in 65% yield by the reaction of Ti(O^{t}Bu)$_4$, $TiCl_4$, and KTp*, followed by treatment with HCl and silica gel chromatography.[18] We found that the reaction of Tp*$TiCl_3$ (**10a**) with 1 equiv of KO^{t}Bu (toluene, 23 °C) yields **11a**, which was isolated as a yellow crystalline solid in 95% yield (eq 2). The aryloxide derivative Tp*Ti(O-2-^{t}Bu-C_6H_4)Cl_2 (**12a**) was prepared by the reaction of **10a** with 1.5 equiv of 2-*tert*-butylphenol and triethylamine in CH_2Cl_2 (eq 2) and was isolated as a red-orange solid in 70% yield.

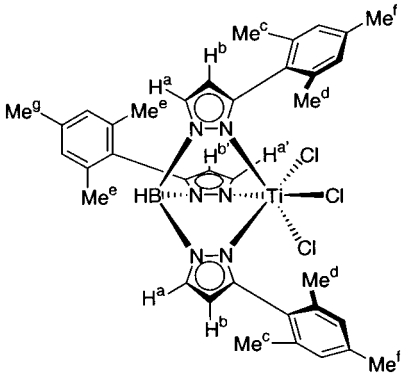

Figure 1. Labeling scheme for Tp*$TiCl_3$ (**10c**).

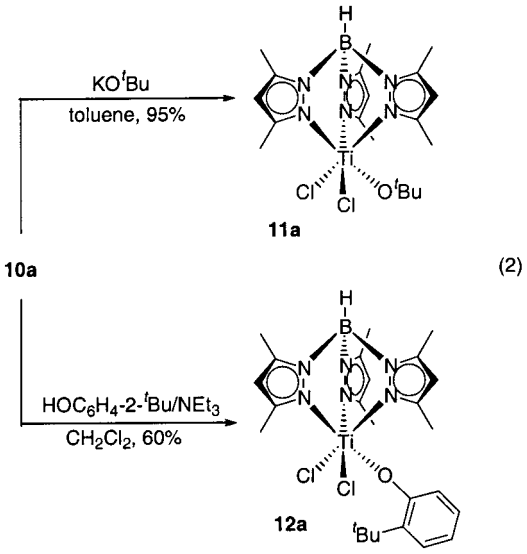

Molecular Structures of Tp′TiX_3 Complexes. The molecular structure of **10a** was recently determined by X-ray crystallography and features a distorted octahedral geometry at titanium with *cis* L−Ti−L angles in the range 83.3(1)−95.2(0)°.[19] We have determined the structure of the *tert*-butoxide analogue **11a** (Figure 2). Crystallographic details and selected bond distances and angles are listed in Tables 1 and 2. The structure of **11a** is very similar to that of **10a**. The *cis* L−Ti−L angles in **11a** are in the range 82.04(9)−97.22(4)°. The Ti−Cl bonds in **11a** (2.318(1) Å average) are slightly longer than those in **10a** (average 2.262(3) Å). The short Ti−O bond distance of 1.741(2) Å and large Ti−O−C(16) bond angle of 165.5(2)° in **11a** are typical for Ti^{IV} alkoxides (cf. $TiCl_2\{\kappa^3$-*C*,*N*,*N*-2,6-$(CH_2NMe_2)_2C_6H_3\}$(O-^{i}Pr) (1.765(2) Å, 149.22(2)°)[20] and $(CpTiCl_2)_2(OCMe_2CMe_2O)$ (1.750(2) Å, 166.2(2)°).[21]

(16) Solid **9c** can be isomerized to **9b** by heating at 236 °C for 1 h (ref 16c). However, the isomerization of **9b** to **9c** has not been reported.
(17) LeCloux, D. D.; Keyes, M. C.; Osawa, M.; Reynolds, V.; Tolman, W. B. *Inorg. Chem.* **1994**, *33*, 6361.
(18) Ipaktschi, J.; Sulzbach, W. *J. Organomet. Chem.* **1992**, *426*, 59.
(19) Antiñolo, A.; Carrillo-Hermosillo, F.; Corrochano, A. E.; Fernández-Baeza, J.; Lanfranchi, M.; Otero, A.; Pellinghelli, M. A. *J. Organomet. Chem.* **1999**, *577*, 174.

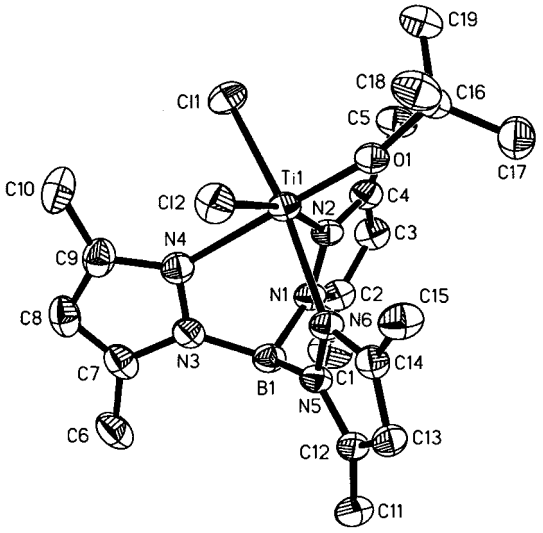

Figure 2. Molecular structure of **11a**. Hydrogen atoms are omitted. Thermal ellipsoids are drawn at the 30% probability level.

Table 1. Summary of Crystallographic Data for Tp*TiCl$_2$(O^{t}Bu)·C$_6$H$_5$Cl (11a·C$_6$H$_5$Cl)

formula	$C_{25}H_{36}BCl_3N_6OTi$
cryst size (mm)	0.35 × 0.18 × 0.05
color, shape	yellow, wedge
cryst syst	triclinic
space group	P1
a, Å	10.6451(2)
b, Å	11.1709(2)
c, Å	13.5833(2)
α, deg	71.777(1)
β, deg	78.134(1)
γ, deg	77.264(1)
V (Å^3)	1480.13(4)
Z	2
μ (mm^{-1})	0.589
diffractometer	Siemens SMART CCD
radiation, *λ* (Å)	0.71073
temp (K)	173(2)
θ range (deg)	1.60 to 25.04
data collected: *h; k; l*	−12,12; −12,13; 0,16
no. of reflns	8459
no. of unique reflns	5057 (R_{int} = 0.0195)
no. of obsd reflns	$I > 2\sigma(I)$, 4131
structure solution	direct methods[a]
refinement	FMLS on F^2
abs corr	SADABS
transmn range (%)	86.9−100
no. of data/restrainsts/params	5057/20/383
R indices ($I > 2\sigma(I)$)[b,c]	R1 = 0.0479, wR2 = 0.1107
R indices (all data)[b,c]	R1 = 0.0630, wR2 = 0.1195

[a] SHELXTL-Plus Version 5.0, Siemens Industrial Automation, Inc., Madison, WI. [b] $R1 = \sum||F_o| - |F_c||/\sum|F_o|$. [c] $wR2 = [\sum[w(F_o^2 - F_c^2)^2]/\sum|[w(F_o^2)^2]]^{1/2}$, where $w = q/\sigma^2(F_o^2) + (aP)^2 + bP$.

To compare the steric properties of the mesityl-substituted complexes **10b** and **10c** and the unsubstituted complex **10e**, space-filling models were generated (Figure 3).[22] It is clear that the Tp ligand of **10e** does not provide significant steric crowding around the $TiCl_3$ unit, whereas the mesityl groups of the Tp^{Ms} ligand in **10b** form a deep pocket. In **10c**, the two Ti−Cl groups that flank the 5-substituted pyrazolyl ring are sterically accessible, while the third Ti−Cl group is more protected.

Table 2. Selected Bond Lengths (Å) and Angles (deg) for Tp*TiCl$_2$(O^{t}Bu) (11a)

Ti−N(4)	2.254 (3)	Ti−Cl(1)	2.333 (9)
Ti−N(6)	2.178 (3)	Ti−Cl(2)	2.31 (1)
Ti−N(2)	2.177 (3)	Ti−O(1)	1.741 (2)
O(1)−Ti−N(6)	96.7(1)	N(6)−Ti−Cl(2)	89.99(7)
N(6)−Ti−N(2)	82.04(9)	N(4)−Ti−Cl(2)	85.87(7)
N(6)−Ti−N(4)	82.8(1)	N(6)−Ti−Cl(1)	166.32(8)
O(1)−Ti−Cl(2)	94.63(8)	N(4)−Ti−Cl(1)	86.16(7)
O(1)−Ti−Cl(1)	94.31(7)	N(5)−N(6)−Ti	121.1(2)
N(2)−Ti−Cl(2)	166.78(8)	N(3)−N(4)−Ti	119.2(2)
N(2)−Ti−Cl(1)	88.62(7)	N(1)−N(2)−Ti	121.0(2)
Cl(2)−Ti−Cl(1)	97.22(4)	O(1)−Ti−N(2)	96.8(1)
Ti−O(1)−C(16)	165.5(2)	O(1)−Ti−N(4)	179.3(1)

Ethylene Polymerization Studies. Activity Trends. The ethylene polymerization behavior of **10a**−**e**, **11a**, and **12a** was investigated in toluene with MAO activation. The results are summarized in Table 3. Sterically open complexes **10e** and **10a** exhibit low activity at 58 °C under the conditions studied (entries 1 and 3), consistent with previous reports.[11a] One possible reason for the low activity of these catalysts is that the MAO reacts with the tris(pyrazolyl)borate B−H bond.[23] However, **10d**, which does not contain a B−H bond, also exhibits low activity (entry 2). Therefore, other factors must contribute to the low activity of **10a**, **10e**, and **10d**. Alkoxide and aryloxide derivatives **11a** and **12a** also exhibit low activity (entries 4 and 5).

Complex **10b**, the most sterically crowded of the catalysts studied, is ca. 50 times more active than **10a**,**d**,**e** (Table 3, entry 6 vs 1−3). Moreover, **10c**, which is somewhat less crowded than **10b**, is ca. 300 times more active than **10a**,**d**,**e** (entry 7 vs 1−3). The activity of **10c** approaches that of Cp_2ZrCl_2 under these conditions (entry 8). For this reason, low catalyst loadings (1 *μ*mol in 80 mL solvent) and short reaction times were used to minimize stirring problems, mass transport limitations, and reaction exotherms. It is clear that steric effects strongly influence the activity of Tp′TiCl$_3$/MAO catalysts, and a moderate degree of steric crowding appears to be optimal.

Effect of Polymerization Conditions. The effects of varying the polymerization conditions were studied for **10c**, which is the most active of the Tp′TiX$_3$ complexes studied. These results are summarized in Table 4.[24] The activity of **10c**/MAO increases by an order of magnitude between 0 and 60 °C, is maximized at ca. 100 °C, and decreases at higher temperatures (entries 9−12).

(20) Donkervoort, J. G.; Jastrzebski, J. T. B. H.; Deelman, B.; Kooijman, H.; Veldman, N.; Spek, A. L.; van Koten, G. *Organometallics* **1997**, *16*, 4174.

(21) Huffman, J. C.; Moloy, K. G.; Marsella, J. A.; Caulton, K. G. *J. Am. Chem. Soc.* **1980**, *102*, 3009.

(22) Titan, version 1.0.1 (Wavefunction), PM3/tm method. The mesityl groups were fixed perpendicular to the pyrazolyl rings. This method was tested for **10a**, and the calculated structural parameters agreed well with the X-ray crystallographic results (ref 19).

(23) (a) Ghosh, P.; Hascall, T.; Dowling, C.; Parkin, G. *J. Chem. Soc., Dalton Trans.* **1998**, 3355. (b) Looney, A.; Han, R.; Gorrell, I. B.; Cornebise, M.; Yoon, K.; Parkin, G.; Rheingold, A. L. *Organometallics* **1994**, *13*, 274. (c) Dowling, C.; Parkin, G. *Polyhedron* **1996**, *15*, 2463. (d) Ghosh, P.; Parkin, G. *Chem. Commun.* **1998**, 413.

(24) The use of different lots of MAO resulted in substantially different activities (e.g., Table 3, entry 7 vs Table 4, entry 10), although structure/activity trends remained unchanged. Increased aging of MAO resulted in increased activity, and the use of the MAO stored at low temperature and then heated for 2 h at 80 °C resulted in higher activity than use of MAO simply stored at low temperature. Others have noted that the source and aging of MAO can impart different cocatalytic characteristics. See: Tritto, I.; Méalares, C.; Sacchi, M. C.; Locatelli, P. *Macromol. Chem. Phys.* **1997**, *198*, 3963.

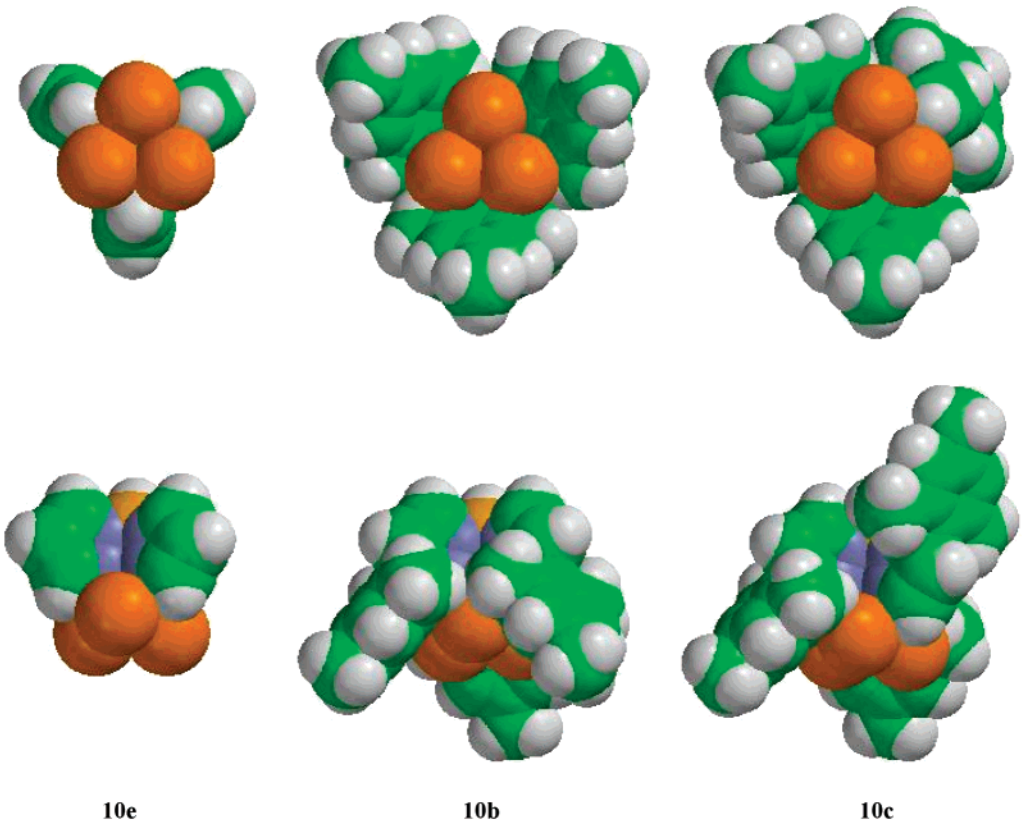

Figure 3. Space-filling models of Tp′$TiCl_3$ complexes.

Table 3. Ethylene Polymerization Results[a]

entry	precatalyst	time (min)	yield (g)[b]	activity [10^6 g polymer/(mol Ti·h·atm)]
1	$TpTiCl_3$ (**10e**)	23	0.052	0.03
2	$BuTpTiCl_3$ (**10d**)	23	0.056	0.03
3	Tp^*TiCl_3 (**10a**)	23	0.064	0.04
4	$Tp^*Ti(O\text{-}tBu)Cl_2$ (**11a**)	23	0.065	0.04
5	$Tp^*Ti(O\text{-}2\text{-}tBu\text{-}C_6H_4)$ (**12a**)	23	0.097	0.06
6	$Tp^{Ms}TiCl_3$ (**10b**)	6	0.70	1.7
7	$Tp^{Ms*}TiCl_3$ (**10c**)	6[c]	3.84	9.1
8	Cp_2ZrCl_2	6[c]	6.39	15

[a] Polymerization conditions: glass Fischer-Porter bottle, 80 mL of toluene, $P_{ethylene}$ = 62 psi, 1 μmol of precatalyst, 960 μmol of MAO (as toluene solution containing 4.67 wt % total Al), T = 58 °C; blank MAO runs were carried out every 5 normal runs. [b] Average of 3 runs; reproducibility of yield and activity is ca. ±10%. [c] Stirring stopped at this time due to polymer precipitation.

Interestingly, **10c**/MAO exhibits higher activity with lower MAO loadings. In fact, **10c**/200 MAO is more active than Cp_2ZrCl_2/1000 MAO or Cp_2ZrCl_2/200 MAO under the conditions studied (entry 13 vs 17,18). This phenomenon has been observed for several other olefin oligomerization and polymerization catalysts.[25] One possible reason for the decrease in activity of **10c**/MAO with increased MAO loadings is that the $AlMe_3$ present in MAO coordinates to the active species, e.g., to form $L_xTi(\mu\text{-}Me)_2AlMe_2^{n+}$ species.[26] Consistent with this supposition, addition of $AlMe_3$ substantially decreases the activity of **10c**/MAO. The use of dried MAO, from which most of the $AlMe_3$ has been removed under vacuum (entry 15), results in higher activity than use of standard MAO solution (which contains 4.7 wt % $AlMe_3$ by NMR, entry 10). Additionally, at high MAO loadings, replacement of 80% of the MAO with $AlMe_3$ decreases the activity substantially (entry 16 vs 14).

Polymer Characterization and Chain Transfer Mechanisms. The polyethylenes produced by **10c**/MAO were analyzed by DSC, NMR, and GPC. DSC analysis shows that the polymers are essentially linear, with T_m = 137 °C for the polyethylene from Table 4, entry 10.

The ^1H NMR spectra of the polyethylenes produced by **10c**/MAO contain methyl end group resonances, but olefin end group resonances are extremely weak or unobservable. For example, the ^1H NMR spectrum of a low molecular weight polymer produced at 100 °C (Table 4, entry 11, M_n = 24 700) is shown in Figure 4 and contains a prominent methyl end group resonance but barely detectable olefinic resonances. These observations suggest that the predominant chain transfer mechanism is alkyl exchange with aluminum[2b,27] (i.e., chain transfer to aluminum, Scheme 3) rather than β-hydride elimination.

The polymers produced by **10c**/MAO exhibit reproducibly broad, multimodal molecular weight distributions (M_w/M_n = 4−15 depending on conditions).[28] Representative gel permeation chromatograms are shown

(25) For example see: (a) Rogers, J. S.; Bazan, G. C. *Chem. Commun.* **2000**, 1209. (b) Herfert, N.; Fink, G. *Makromol. Chem.* **1992**, *193*, 1359. (c) Herfert, N.; Fink, G. *Makromol. Chem. Macromol. Symp.* **1993**, *66*, 157. (d) Jüngling, S.; Mülhaupt, R. *J. Organomet. Chem.* **1995**, *497*, 27. (e) Fink, G.; Herfert, N.; Montag, P. In *Ziegler Catalysis*; Fink, G., Mülhaupt, R., Brintzinger, H. H., Eds.; Springer-Verlag: Berlin, 1995; p 159. (f) Kleinschmidt, R.; v. d. Leek, Y.; Reffke, M.; Fink, G. *J. Mol. Catal. A* **1999**, *148*, 29.

(26) (a) Bochmann, M.; Lancaster, S. J. *Angew. Chem., Int. Ed. Engl.* **1994**, *33*, 1634. (b) Kim, I.; Jordan, R. F. *Macromolecules* **1996**, *29*, 489. (c) Tritto, I.; Donetti, R.; Sacchi, M. C.; Locatelli, P.; Zannoni, G. *Macromolecules* **1997**, *30*, 1247. (d) Coevoet, D.; Cramail, H.; Deffieux, A.; Mladenov, C.; Pedeutour, J.-N.; Peruch, F. *Polym. Int.* **1999**, *48*, 257, and references therein. (e) Pédeutour, J.-N.; Coevoet, D.; Cramail, H.; Deffieux, A. *Macromol. Chem. Phys.* **1999**, *200*, 1215.

Table 4. Effect of Conditions on Polymerization by $Tp^{Ms*}TiCl_3$ (10c)/MAO[a]

entry	precatalyst	equiv MAO	equiv added $AlMe_3$	temp (°C)	time (min)	activity [10^6 g polymer/(mol Ti·h·atm)]	M_p ($\times 10^3$)[b]
9	**10c**	1000	0	0	6	0.17	1540
10	**10c**	1000	0	60	6	2.9	85.8
11	**10c**	1000	0	100	6	4.7	24.7
12[c]	**10c**	1000	0	130	6	3.6	12.1
13	**10c**	200	0	60	0.75[d]	7.4	1430
14	**10c**	5000	0	60	6	0.70	68.2
15	**10c**	1000, dried[e]	0	60	6	4.3	239
16	**10c**	1000	4000	60	6	0.22	20.0
17	Cp_2ZrCl_2	1000	0	60	4[d]	6.3	442
18	Cp_2ZrCl_2	200	0	60	6	5.6	

[a] Polymerization conditions (unless otherwise noted): glass Fischer-Porter bottle, 80 mL of toluene, $P_{C2H4} = 60$ psi, 1 μmol of precatalyst, MAO solution in toluene (13.48 wt % total Al). [b] Peak molecular weight determined by GPC, reported vs narrow polystyrene standards, obtained in 1,2,4-trichlorobenzene at 150 °C. [c] $P_{ethylene} = 50$ psi. [d] Reaction stopped stirring at this time due to polymer precipitation. [e] MAO was stripped of volatiles prior to use.

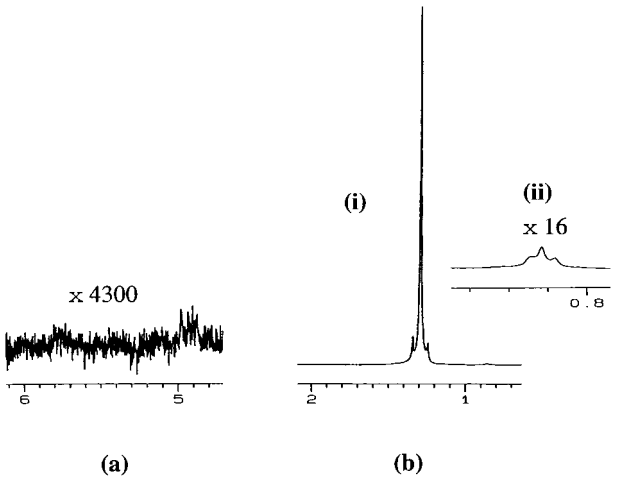

Figure 4. ^{1}H NMR spectrum (110 °C, 1,2-$C_6H_4Cl_2$) of polyethylene from Table 4, entry 11. (a) Olefinic region. (b) Polymer main chain (i) and methyl end group (ii) resonances.

Scheme 3

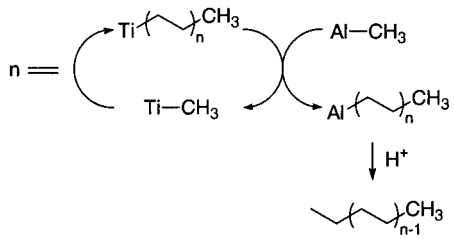

in Figure 5. Broad polydispersities can occur if more than one active species is present, or if the ratio of the chain propagation rate to the chain transfer rate (R_{prop}/R_{trans}) changes during the time of polymerization. The latter situation can arise if the concentration and/or structure of the chain transfer agent changes during the course of the polymerization.

To probe the possibility of chain transfer to aluminum and the origin of the broad molecular weight distributions, the influence of the MAO concentration on molecular weight was studied. As summarized in Table 4 and Figure 5, molecular weights decrease as the MAO concentration is increased. For example, when the MAO/Ti ratio is increased from 200 to 1000 by increasing [MAO] at constant [Ti], the peak molecular weight M_p decreases from 1 430 000 to 85 800 (entry 13 vs 10). The M_p value decreases further to 68 200 when the MAO/Ti ratio is increased to 5000 (entry 14). This trend is consistent with efficient chain transfer to aluminum.

Increasing the MAO concentration also narrows the molecular weight distribution of the major polymer fraction (Figure 5). The polymer produced by **10c**/200 MAO (entry 13) has a very broad molecular weight distribution ($M_w/M_n = 7$). In contrast, the polymer produced by **10c**/5000 MAO (entry 14) comprises a major, low molecular weight fraction with M_w/M_n = ca. 3.5 and a minor, high molecular weight fraction. These result are consistent with extensive chain transfer to aluminum, since changes in R_{prop}/R_{trans} during the time of polymerization are less significant when higher initial aluminum concentrations are used. The ratio (mol total Al-Me)$_{initial}$/(mol chains produced) is ca. 18 and 350 for entries 13 and 14, respectively.[29]

Identification of Predominant Chain Transfer Agent. To probe the question of whether the chain transfer involves MAO or the $AlMe_3$ contained in the MAO, the influence of cocatalyst composition was studied. As shown in Table 4 and Figure 5, the **10c**/1000 MAO catalyst prepared from MAO solution produces polyethylene with $M_p = 85\,800$ at 60 °C (entry 10). However, the use of 1000 equiv of dried MAO, from which most of the $AlMe_3$ has been removed under vacuum, results in substantially higher molecular weight ($M_p = 239\,000$, entry 15). In contrast, addition of 4000 equiv of $AlMe_3$ to the **10c**/1000 MAO catalyst decreases

(27) (a) Resconi, L.; Piemontesi, F.; Granciscono, G.; Abis, L.; Fiorani, T. *J. Am. Chem. Soc.* **1992**, *114*, 1025. (b) Mogstad, A.-L.; Waymouth, R. M. *Macromolecules* **1992**, *25*, 2282. (c) Rieger, B.; Reinmuth, A.; Röll, W.; Brintzinger, H. H. *J. Mol. Catal.* **1993**, *82*, 67. (d) Leino, R.; Luttikhedde, H. J. G.; Lehmus, P.; Wilén, C.-E.; Sjöholm, R.; Lehtonen, A.; Seppälä, J. V.; Näsman, J. H. *Macromolecules* **1997**, *30*, 3477. (e) Byun, D.-J.; Shin, D.-K.; Kim, S. Y. *Polym. Bull.* **1999**, *42*, 301. (f) Byun, D.-J.; Shin, D.-K.; Kim, S. Y. *Macromol. Rapid Commun.* **1999**, *20*, 419. (g) Byun, D.-J.; Kim, S. Y. *Macromolecules* **2000**, *33*, 1921. (h) Barsties, E.; Scheible, S.; Prosenc, M.-H.; Rief, U.; Röll, W.; Weyand, O.; Dorer, B.; Brintzinger, H.-H. *J. Organomet. Chem.* **1996**, *520*, 63. (i) Przylbyla, C.; Fink, G. *Acta Polym.* **1999**, *50*, 77.

(28) Polyethylenes produced by **10a**/MAO and **10e**/MAO also exhibited broad polydispersities. See ref 11a.

(29) The ratio of total Al-Me groups from MAO and the $AlMe_3$ contained therein (assuming MAO = (Al(Me)−O)$_n$) to polymer chains produced was calculated according to the following: (mol total Al-Me groups)/(mol polymer chains) = (mol total Al-Me groups)(M_n)/(g polymer yield). M_n was determined versus polystyrene standards by GPC using the Universal Calibration method (polystyrene: $K = 14.1 \times 10^{-5}$, $\alpha = 0.700$; polyethylene: $K = 40.6 \times 10^{-5}$, $\alpha = 0.725$). M_n values determined by this method closely approximated values calculated from ^{1}H NMR spectra of the low molecular weight polymers (assuming all end groups are methyl). For the polymers produced in Table 4, the values for M_n and (mol total Al-Me)initial/(chains produced) are as follows: Entry 10: 17,100; 43. Entry 13: 63,100; 18. Entry 14: 15,900; 350. Entry 15: 102,700; 56. Entry 16: 3,120; 420.

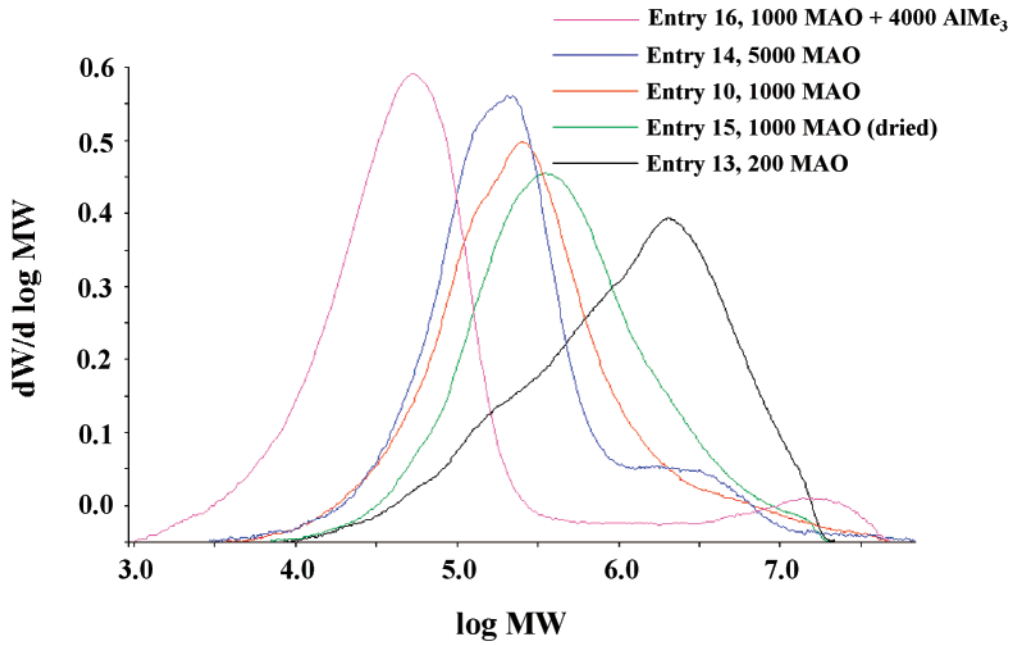

Figure 5. Gel permeation chromatograms (1,2,4-trichlorobenzene, 150 °C) of polyethylenes synthesized using **10c** and varied cocatalyst packages. Entry designations refer to Table 4.

M_p to 20 000 (entry 16). For comparison, addition of 4000 equiv of MAO to the **10c**/1000 MAO catalyst (MAO/**10c** = 5000) decreases M_p to 68 200 (entry 14). These results are consistent with predominant chain transfer to $AlMe_3$.[30]

Evidence for Multiple Active Species. Addition of $AlMe_3$ to the **10c**/MAO catalyst also results in a narrowing of the molecular weight distribution. For example, as illustrated in Figure 5, the polymer from entry 16 comprises a major low molecular weight fraction (M_p = 20 000) for which M_w/M_n = ca. 3, and a minor high molecular weight fraction (M_p = ca. 8 000 000; M_w/M_n = ca. 4−5).[31] For this entry, the ratio (mol total Al-Me)$_{initial}$/(mol chains produced) is ca. 420, and the ratio (mol $AlMe_3$)$_{initial}$/(mol chains produced) is ca. 130;[32] that is, under these conditions, the chain transfer does not significantly decrease the Al-Me concentration during the course of the polymerization. Thus, in this case, the observation of low and high molecular weight fractions strongly suggests that several active species are present: one that undergoes efficient chain transfer to $AlMe_3$ and one (or more) that does (do) not.

Comparative Studies of $TiCl_4$/MAO and $TiCl_3$/MAO Catalysts. One possible explanation for the high activity of **10b**/MAO and **10c**/MAO is that the bulky Tp^{Ms} and Tp^{Ms*} ligands are displaced from Ti under the polymerization conditions, resulting in a classic Ziegler catalyst. To probe this issue, ethylene polymerizations were performed using $TiCl_3$/MAO and $TiCl_4$/MAO under conditions analogous to entry 10. The $TiCl_3$/1000 MAO and $TiCl_4$/1000 MAO catalysts exhibited much lower activity than **10b**/MAO or **10c**/MAO and produced polymer of much higher molecular weight than that produced by **10c**. In addition, the polymer produced by $TiCl_4$/MAO exhibited distinct vinyl end groups in the ^{1}H NMR spectrum, despite the higher molecular weight. As noted above, the polymers produced by **10c** contain virtually no vinyl end groups. From these differences we conclude that the Tp′ ligand is retained in the active species, although partial dissociation cannot be ruled out.

Nature of the Active Species Derived from 10c/MAO. The conventional view of the activation of L_nMX_2 species by MAO invokes generation of coordinatively unsaturated L_nMR^+ species by alkylation and X^- abstraction reactions.[33] In the case of titanium and other reducible metals, further chemistry can occur to generate reduced species, e.g. $L_{n-1}MR^+$, as implicated for $CpTiX_3$-based catalysts.[34] The available data for Tp′TiX_3/MAO catalysts are very limited at present. The present results suggest that the Tp′ ligand remains coordinated to titanium in the active species. The active species is probably a low-coordinate Tp′Ti alkyl species, since bulky Tp′ ligands enhance activity and the addition of $AlMe_3$ decreases activity. XPS core binding energy data indicate that most of the Ti remains as Ti(IV) under polymerization conditions.[35] Efforts to prepare discrete Tp′TiR_2^+ species, which are reasonable

(30) (a) Michelotti, M.; Altomare, A.; Ciardelli, F.; Ferrarini, P. *Polymer* **1996**, *37*, 5011. (b) D'Agnillo, L.; Soares, J. B. P.; Penlidis, A. *Macromol. Chem. Phys.* **1998**, *199*, 955. (c) Rieger, B.; Janiak, C. *Angew. Makromol. Chem.* **1994**, *215*, 35. (d) Naga, N.; Mizuma, K. *Polymer* **1998**, *39*, 5059. (e) Resconi, L.; Fait, A.; Piemontesi, F.; Colonnesi, M.; Rychlicki, H.; Ziegler, R. *Macromolecules* **1995**, *28*, 6667.

(31) Because the upper limit of the molecular weight distribution falls outside the range of the calibration standards, these data are only approximate. The shape and intensity of this minor peak also varied between runs.

(32) The estimated ratio of mol $AlMe_3$ (including that contained in MAO) to mol polymer chains produced was calculated in an analogous way to that in ref 29. For the polymers produced in Table 4, the values for (mol $AlMe_3$)initial/(mol chains produced) are as follows: entry 10: 4; entry 13: 2; entry 14: 35; entry 15: 0; entry 16: 130.

(33) Guram, A. S.; Jordan, R. F. In *Comprehensive Organometallic Chemistry*, 2nd ed.; Lappert, M. F., Ed.; Pergamon/Elsevier: Oxford, 1995; Vol. 4, p 589, and references therein.

(34) (a) Grassi, A.; Saccheo, S.; Zambelli, A.; Laschi, F. *Macromolecules* **1998**, *31*, 5588. (b) Pellecchia, C.; Grassi, A. *Top. Catal.* **1999**, *7*, 125. (c) Grassi, A.; Zambelli, A. *Organometallics* **1996**, *15*, 480. (d) Zambelli, A.; Pellecchia, C.; Oliva, L. *Makromol. Chem., Macromol. Symp.* **1991**, *48−49*, 297.

(35) Gil, M. P.; dos Santos, J. H. A.; Casagrande, O. L., Jr. *Macromol. Chem. Phys.* **2001** *202*, 319.

candidates for the active species in the $Tp'TiX_3$/MAO catalysts, have been unsuccessful to date because the parent $Tp'TiR_3$ complexes are thermally unstable.

Conclusions

The following conclusions emerge from this initial study of the ethylene polymerization performance of $Tp'TiX_3$/MAO catalysts. (i) The activity of $Tp'TiX_3$/MAO catalysts is very sensitive to the steric properties of the Tp′ ligands. The highest activity is exhibited by moderately crowded catalysts containing bulky substituents at the 3-position of two of the three pyrazolyl rings, i.e., $Tp^{Ms*}TiCl_3$/MAO (**10c**/MAO).[36] (ii) The predominant chain transfer mechanism for **10c**/MAO is chain transfer to the $AlMe_3$ contained in the MAO, which results in broad molecular weight distributions when low (**10c**/200 MAO) or moderate (**10c**/1000 MAO) MAO loadings are used. (iii) When high Al loadings are used (**10c**/5000 MAO or **10c**/1000 MAO/4000 $AlMe_3$), bimodal molecular weight distributions comprising a major low molecular weight fraction (M_w/M_n = ca. 3) and a minor high molecular weight fraction are obtained. These results suggest that several active species are present: one that undergoes efficient chain transfer to $AlMe_3$ and one (or more) that does (do) not. (iv) As $TiCl_4$/MAO and $TiCl_3$/MAO produce polymers with distinctly different properties compared to those produced by **10c**/MAO, it is likely that the Tp^{Ms*} ligand is retained in the active species.

Experimental Section

General Procedures. All manipulations were performed using standard vacuum line, Schlenk, or glovebox techniques under a purified N_2 atmosphere. Benzene, hexane, THF, and diethyl ether were distilled from sodium benzophenone ketyl, and CH_2Cl_2 was distilled from P_2O_5. Toluene was distilled from sodium benzophenone ketyl or dried by passage through columns of activated alumina and BASF R3-11 oxygen removal catalyst. Solvents were stored under N_2 or vacuum prior to use. Potassium *tert*-butoxide, $TiCl_4$ (1 M solution in CH_2Cl_2), and 2-*tert*-butylphenol were purchased from Aldrich and used as received. The compounds K[Tp*],[13b] Tl[Tp^{Ms}],[13c] Tl[Tp^{Ms*}],[13c] Na[^{Bu}Tp],[13a] and $TpTiCl_3$ (**10e**)[14] were prepared by literature procedures. Compounds **10a**−**e**, **11a**, and **12a** are air-stable as solids but are moderately air sensitive in solution. MAO for the polymerizations listed in Table 3 was obtained as a 4.67 wt % Al solution in toluene from Albemarle, stored at room temperature, and used without further purification. MAO for chain transfer experiments listed in Table 4 was obtained from Albemarle as a 13.48 wt % Al solution in toluene, stored at −30 °C, and used without further purification.

NMR spectra for titanium complexes were recorded on a Bruker AMX-360 spectrometer in Teflon-valved NMR tubes at ambient probe temperature. Chemical shifts are reported versus $SiMe_4$ and were determined by reference to the residual ^1H and ^{13}C solvent peaks. Coupling constants are reported in hertz. ^1H NMR spectra of polyethylene samples were recorded on a Bruker DRX-400 spectrometer at 110 °C in 1,2-$C_6D_4Cl_2$, and spectra were referenced versus hexamethyldisiloxane (0.7 ppm). Chemical shifts are reported versus $SiMe_4$. Mass spectra were obtained using the direct insertion probe method on a VG Analytical Trio I instrument operating at 70 eV. Gel permeation chromatography was performed on a Polymer Laboratories PL-GPC 220 using 1,2,4-trichlorobenzene solvent (stabilized with 125 ppm BHT) at 150 °C. A set of three PLgel 10 μm Mixed-B or Mixed-B LS columns was used. Samples were prepared at 165 °C and filtered through 2 or 5 μm stainless steel frits prior to injection. Elemental analyses were performed by Desert Analytics Laboratory.

Tp*TiCl$_3$ (10a).[14] A slurry of KTp* (5.30 g, 15.8 mmol) in THF (80 mL) was cooled to 0 °C, and $TiCl_4$ (1.76 mL, 15.8 mmol) was added dropwise. The resulting orange suspension was stirred and refluxed overnight. The solvent was removed under vacuum, and the crude orange product was extracted with benzene (200 mL) for 36 h in a Soxhlet apparatus. The orange benzene extract was cooled to room temperature and filtered, yielding a bright orange solid (5.70 g, 80% based on KTp*). ^1H NMR ($CDCl_3$): δ 5.78 (s, 3H, pz H-4), 2.75 (s; 9H; Me), 2.37 (s; 9H; Me). IR (KBr): ν_{B-H} 2559 cm^{-1}.

Tp^{Ms}TiCl$_3$ (10b). A solution of $TiCl_4$ in CH_2Cl_2 (1.30 mL, 1 M, 1.30 mmol) was added dropwise by syringe to a suspension of $TlTp^{Ms}$ (1.00 g, 1.30 mmol) in CH_2Cl_2 (40 mL) at room temperature. The resulting cloudy yellow mixture was stirred overnight. The reaction mixture was filtered by cannula, and the filtrate was dried under vacuum to afford an orange solid. This material was recrystallized from hot THF (0.60 g, 64% based on $TlTp^{Ms}$). Anal. Calcd for $C_{36}H_{40}BCl_3N_6Ti$: C, 59.87; H, 5.54; N, 11.64. Found: C, 59.66; H, 5.46; N, 11.52. ^1H NMR ($CDCl_3$): δ 7.84 (d, 3H; $^3J_{HH}$ = 2.1, pz 5-H), 6.76 (s, 6H, Ph 3-H and 5-H), 6.09 (d, 3H, $^3J_{HH}$ = 2.1, pz 4-H), 2.21 (s, 9H, mesityl *para*-Me), 1.90 (s, 18H, mesityl *ortho*-Me). $^{13}C\{^1H\}$ NMR ($CDCl_3$): δ 156.9 (pz 3-C), 138.0 (Ph 4-C), 137.9 (Ph 2-C and 6-C), 135.6 (pz 5-C), 130.1 (Ph 1-C), 127.5 (Ph 3-C and 5-C), 107.3 (pz 4-C), 21.4 (mesityl *para*-Me), 20.80 (mesityl *ortho*-Me). IR (KBr): ν_{B-H} 2500 cm^{-1}. EI-MS [*m*/*z*]: 686 [M − Cl].

Tp^{Ms*}TiCl$_3$ (10c). Method A. A solution of $TlTp^{Ms}$ (6.84 g, 8.86 mmol) in THF (80 mL) was prepared, a solution of $TiCl_4$·2THF (2.95 g, 8.83 mmol) in THF (80 mL) was added by cannula, and the resulting orange slurry was stirred for 16 h at room temperature. The solvent was removed under vacuum to afford an orange solid, which was extracted with toluene. The toluene extract was filtered through Celite and concentrated to ∼50 mL (slurry). Approximately 300 mL of pentane was added, turning the slurry bright yellow. The mixture was stored at −80 °C for several hours, resulting in more yellow precipitate. The precipitate was collected by filtration, washed with pentane, and dried under vacuum to yield a yellow powder (4.78 g, 75%). The product can be crystallized in THF/pentane or hot octane. Anal. Calcd for $C_{36}H_{40}BCl_3N_6Ti$: C, 59.87; H, 5.54; N, 11.64. Found: C, 59.61; H, 5.39; N, 11.45. ^1H NMR ($CDCl_3$): δ 8.35 (d, 1H, $^3J_{HH}$ = 2.1, pz 3-H), 7.63 (d; 2H; $^3J_{HH}$ = 2.1, pz 5-H), 7.01 (s; 2H; Ph H), 6.90 (s; 2H; Ph H), 6.88 (s; 2H; Ph H), 6.12 (d; 1H; $^3J_{HH}$ = 2.1; pz 4-H), 6.04 (d; 2H; $^3J_{HH}$ = 2.1, pz 4-H), 2.41 (s; 3H; mesityl *para*-Me), 2.28 (s; 6H; mesityl *para*-Me), 1.94 (s; 6H; mesityl *ortho*-Me), 1.92 (s; 6H; mesityl *ortho*-Me), 1.90 (s; 6H; mesityl *ortho*-Me). $^{13}C\{^1H\}$ NMR ($CDCl_3$): δ 157.7 (pz 3-C), 146.4 (3-C pz), 139.8, 139.2, 138.9, 138.6, 138.4, 136.9, 131.1, 128.7, 128.5, 128.3 (aromatic carbons and 5-C pz), 107.9 (pz 4-C), 106.7 (pz 4-C) 21.8 (mesityl *ortho*-Me), 21.9 (mesityl *ortho*-Me), 20.3 (mesityl *ortho*-Me). IR (KBr): ν_{B-H} 2530 cm^{-1}. EI-MS [*m*/*z*]: 722.194 [M^+].

Method B. A solution of $TiCl_4$ in CH_2Cl_2 (1.30 mL, 1 M, 1.30 mmol) was added dropwise to a solution of $TlTp^{Ms*}$ (1.00 g, 1.30 mmol) in CH_2Cl_2 (40 mL) at room temperature. The cloudy orange mixture was stirred overnight. The solvent was removed under vacuum to afford an orange solid. The crude orange solid was dissolved in hot benzene and filtered, and the solvent was removed from the filtrate under vacuum to give an orange-yellow solid (0.63 g, 70% based on $TlTp^{Ms*}$).

^{Bu}TpTiCl$_3$ (10d). A solution of Na[^{Bu}Tp] (2.00 g, 6.85 mmol) in CH_2Cl_2 (80 mL) was cooled to 0 °C. A solution of $TiCl_4$ in CH_2Cl_2 (6.85 mL, 1 M, 6.85 mmol) was added dropwise, and the resulting orange suspension was stirred for 16 h. The

(36) This trend extends to Zr and V catalysts. (a) Furlan, L. G.; Gil, M. P.; Casagrande, O. L., Jr. *Macromol. Rapid Commun.* **2000**, *21*, 1054. (b) Casagrande, O. L., Jr.; Casagrande, A. C. A.; Swenson, D. C.; Young, V. G., Jr.; Jordan, R. F. Manuscript in preparation.

solvent was removed under vacuum, and the crude yellow product was dissolved in hot benzene (80 mL) and filtered. The solvent was removed from the filtrate under vacuum to afford a yellow solid (2.0 g, 70% based on Na[^{Bu}Tp]). Anal. Calcd for $C_{13}H_{18}BCl_3N_6Ti$: C, 36.83; H, 4.25; N, 19.83; Ti, 11.30. Found: C, 36.20; H, 4.38; N, 17.63; Ti, 11.82. ^{1}H NMR ($CDCl_3$): δ 8.08 (d; 3H; $^3J_{HH}$ = 2.2, pz 3-H), 7.47 (d; 3H; $^3J_{HH}$ = 2.2, pz 5-H), 6.07 (t, 3H, $^3J_{HH}$ = 2.2, pz 4-H), 1.50−1.31 (m, 9H, Bu). ^{13}C{^{1}H} NMR ($CDCl_3$): δ 145.3 (pz 2-C), 122.5 (pz 5-C), 104.62 (pz 4-C), 27.4 (CH_2, Bu), 26.9 (CH_2, Bu), 14.07 (CH_2, Bu). EI-MS [*m*/*z*]: 422.024 [M^+].

Tp*Ti(O^{t}Bu)Cl$_2$ (11a).[18] A slurry of Tp*$TiCl_3$ (2.00 g, 4.42 mmol) and KO^{t}Bu (0.500 g, 4.42 mmol) in toluene (100 mL) was stirred overnight at room temperature. The mixture was filtered by cannula. The filtrate was dried under vacuum to afford a yellow solid (2.05 g, 95%). Crystals were grown by slow evaporation of a C_6H_5Cl solution at room temperature. ^{1}H NMR (CD_2Cl_2): δ 5.60 (s; 1H; pz 4-H), 5.50 (s; 2H; pz 4-H); 2.21 (s; 3H; pz Me), 2.14 (s; 6H; pz Me), 2.08 (s; 3H; pz Me), 2.05 (s; 6H; pz Me), 1.80 (s, 9H, O^{t}Bu). IR (KBr): ν_{B-H} 2549 cm^{-1}.

Tp*Ti(O-2-^{t}Bu-C$_6$H$_4$)Cl$_2$ (12a). A flask was charged with Tp*$TiCl_3$ (1.00 g, 2.22 mmol) and CH_2Cl_2 (40 mL), and 2-*tert*-butylphenol (0.22 mL, 2.2 mmol) was added at room temperature, yielding an orange suspension. Triethylamine (0.46 mL, 2.2 mmol) was added by syringe, and the mixture was stirred for 2 h to give a dark red solution. The volatiles were removed under vacuum, and the resulting orange solid was extracted with toluene (2 × 20 mL). The combined extract was evaporated under vacuum to give a red-orange powder that was dried under vacuum at 150 °C for 6 h (0.75 g, 60%). Anal. Calcd for $C_{25}H_{24}BCl_2N_6OTi$: C, 52.10; H, 6.19; N, 14.87. Found: C, 52.22; H, 5.90; N, 14.55. ^{1}H NMR (CD_2Cl_2): δ 7.28 (dd, 1H, $^2J_{HH}$ = 7.9, $^5J_{HH}$ = 1.5, Ph 2-H), 6.88 (dt, 1H, $^3J_{HH}$ = 8.0, $^5J_{HH}$ = 1.1, Ph 4-H), 6.66 (dt, 1H, $^3J_{HH}$ = 7.6, $^5J_{HH}$ = 1.2, Ph 5-H), 5.84 (s; 1H; pz 4-H), 5.65 (s; 2H; pz 4-H), 5.41 (dd, 1H, $^3J_{HH}$ = 8.0, $^5J_{HH}$ = 1.0, Ph 6-H), 2.88 (s; 3H; pz Me), 2.42 (s; 6H; pz Me), 2.29 (s; 3H; pz Me), 1.99 (s; 6H; pz Me), 1.72 (s, 9H, ^{t}Bu). ^{13}C{^{1}H} NMR (CD_2Cl_2): δ 162.9 (O*C*Ph), 152.6 (pz 2-C), 150.84 (pz 2-C), 142.0 (pz 5-C), 141.6 (pz 5-C), 126.8 (Ph H), 125.4 (Ph H), 122.4 (Ph H), 122.6 (Ph H), 105.7 (pz 4-C), 105.2 (pz 4-C), 22.7 (*C*(CH$_3$)$_3$), 29.6 (C(*C*H$_3$)$_3$), 15.0 (pz 2-Me), 12.2 (pz 2-Me), 11.1 (pz 5-Me), 11.0 (pz 5-CH$_3$). IR (KBr): ν_{B-H} 2550 cm^{-1}. EI-MS [*m*/*z*]: 564.182 [M^+].

Ethylene Polymerizations (Table 3). Polymerization reactions were performed in a 100 or 200 mL Fischer-Porter bottle equipped with a magnetic stir bar and a stainless steel pressure head fitted with inlet and outlet needle valves, a septum-capped ball valve for injections, a check valve for safety, and a pressure gauge. In a glovebox, the bottle was charged with MAO and 60 mL of dry toluene and sealed. The bottle was removed from the glovebox and attached to a stainless steel double manifold (vacuum/ethylene) line. The nitrogen atmosphere was removed by vacuum, and the solution was saturated with ethylene and thermally equilibrated at 58 °C for 10 min. The polymerization reactions were started by addition of a solution of the titanium complex in dry toluene (20 mL), followed by an immediate increase of the ethylene pressure to 62 psi. The total volume of the reaction mixture was 80 mL for all polymerization reactions. The total pressure was kept constant by feeding ethylene on demand. After the specified reaction time, the polymerization was stopped by cooling and venting of the reaction vessel, followed by quenching of the reaction with methanol. The polymer was washed with acidic ethanol or methanol for several hours, then washed with methanol and dried under vacuum for 12 h.

Ethylene Polymerizations (Table 4). The procedure was identical to that for the Table 3 runs, except that MAO was initially charged with 78 mL of dry toluene, and the titanium precatalyst was injected as a 2 mL solution. In addition, the reaction temperature and ethylene pressure were 60 °C and 60 psi, respectively, unless otherwise noted.

Acknowledgment. This work was supported by U.S. Department of Energy and OPP Petrochemical SA (Brazil). O.L.C. acknowledges the CNPq (Brazil) for a fellowship. The X-ray diffraction analysis of **11a** was performed by Victor G. Young, Jr. at the X-ray Crystallographic Laboratory of the University of Minnesota Department of Chemistry. We also thank Dr. Andrey Korolev (University of Chicago) for valuable suggestions and Dr. William Beard (Albemarle Chemical) for helpful discussions and gifts of MAO.

Supporting Information Available: Tables of atomic coordinates, isotropic displacement parameters, anisotropic displacement parameters, bond distances and bond angles, and hydrogen atom coordinates for **11a**·C_6H_5Cl. This material is available free of charge via the Internet at http://pubs.acs.org.

OM010530J